Carbohydrate Polymers 115 (2015) 636–642

Contents lists available at ScienceDirect

Carbohydrate Polymers

journal homepage: www.elsevier.com/locate/carbpol

Preparation and characterization of BC/PAM-AgNPs nanocomposites for antibacterial applications

Guang Yang[a,b,*], Caixia Wang[a], Feng Hong[a,*], Xuexia Yang[a], Zhangjun Cao[a]

[a] College of Chemistry, Chemical Engineering and Biotechnology, Donghua University, North Ren Min Road No. 2999, Shanghai 201620, PR China
[b] Key Laboratory of Science & Technology of Eco-Textile, Donghua University/Jiangnan University, Ministry of Education, Shanghai 201620, PR China

ARTICLE INFO

Article history:
Received 24 June 2014
Received in revised form 3 September 2014
Accepted 6 September 2014
Available online 28 September 2014

Keywords:
Bacterial cellulose
Polyacrylamide
Silver nanoparticles
Template synthesis
Antibacterial activity

ABSTRACT

In this work, a bacterial cellulose/polyacrylamide (BC/PAM) double network composite was prepared to act as the template for in situ synthesis of silver nanoparticles (AgNPs). Effects of reaction conditions of the BC/PAM composite were investigated on its microstructure, mechanical properties and thermal stabilities. Both the BC/PAM composite and pure BC were utilized to prepare the corresponding silver impregnated nanocomposites, i.e., BC/PAM-AgNPs and BC-AgNPs, by an environmental friendly method, UV irradiation. The influences of the templates were investigated on the AgNPs formation and the antibacterial activities of the nanocomposites by both the zone of inhibition and dynamic shake flask methods. It was shown that the BC/PAM composite displayed a denser microstructure and higher thermal stabilities than pure BC. The BC/PAM-AgNPs nanocomposite exhibited a bigger particle size and lower mass content of AgNPs than the BC-AgNPs one. For the antibacterial test, two nanocomposites exhibited a close antibacterial effect, with a high log reduction above 3 and killing ratio above 99.9%, respectively.

1. Introduction

Bacterial cellulose, a kind of novel cellulose material produced by microbes, has attracted more and more attentions for its distinctive micro- and nano-structure and physical properties, e.g., 3-D structure consisting of an ultrafine network of cellulose nanofibers, high purity and free of lignin and hemicelluloses, high porosity as well as good biocompatibility, making it a suitable candidate for producing high quality paper, sewage purification and various biomedical materials such as temporary wound dressing (Czaja, Krystynowicz, Bielecki, & Brown, 2006). On the other hand, functional nanocomposites based on polymers and nanoscale fillers have been focused in both scientific and industrial applications for their functionality improvement (Jiang, Zhou, Li, Wang, & Xie, 2006a; Jiang et al., 2006b; Bao, Xu, Li, & Li, 2010; Li, Bao, & Li, 2011). In recent years, various types of nanoparticles were reported to be assembled on the surfaces of cellulose fibers to supply functionalities, such as antibacterial or catalytic activity and external colors (Cheng, Hung, Chen, & Young, 2014; Saleh & Djaja, 2014; Cai, Kimura, Wada, & Kuga, 2009). Among them, silver nanoparticles (AgNPs) are one of the most effective antibacterial and catalytic agents because of their large surface area to volume ratio as well as surface plasmon resonance (Rai, Yadav, & Gade, 2009). Now, AgNPs containing products have been commercialized in broad application fields, such as textile (El-Rafie, Ahmed, & Zahran, 2014), wound dressing (Yang, Xie, Deng, Bian, & Hong, 2012a), water and air purification (Bryaskova et al., 2014) and self-sterilizing polymer films (Loher, Schneider, Maienfisch, Bokorny, & Stark, 2008). In our previous work, we have explored a kind of silver nanoparticle impregnated bacterial cellulose (BC-AgNPs) nanocomposite (Yang et al., 2012a; Yang, Xie, Hong, Cao, & Yang, 2012b), which showed a prominent antibacterial activity.

But pure BC exhibited an insufficiently high level of mechanical properties, which hindered its broad use in practical applications including BC based composites. In recent years, the semi-interpenetrating network (semi-IPN) technique has been proposed to prepare the double network gels (DN gels), which are characterized by a special network structure consisting of two types of polymer components. It has been reported that the DN gels produced from many different polymer pairs exhibited much better mechanical properties than that from individual component (Hagiwara, Putra, Kakugo, Furukawa, & Gong, 2010; Gong, Katsuyama, Kurokawa, & Osada, 2003; Buyanov, Gofman, Revel'skaya, Khripunov, & Tkachenko, 2010).

* Corresponding authors at: College of Chemistry, Chemical Engineering and Biotechnology, Donghua University, North Ren Min Road No. 2999, Shanghai 201620, China. Tel.: +86 21 6779 2749/86 21 6779 2649;
fax: +86 21 6779 2749/86 21 6779 2649..
E-mail addresses: gyang@dhu.edu.cn (G. Yang), fhong@dhu.edu.cn (F. Hong).

http://dx.doi.org/10.1016/j.carbpol.2014.09.042
0144-8617/

Considering the natural 3-D structure of nanofiber network from BC material, in this work, we proposed to combine BC as the first network, with polyacrylamide (PAM) as the second network, via free radical polymerization to prepare a bacterial cellulose/polyacrylamide (BC/PAM) DN gel material. Polyacrylamide is an acrylate polymer (—$CH_2CHCONH_2$—) formed by cross-linking of acrylamide subunits, and has been widely used in the fields of biomedical applications (Lee, Tettey, Kim, Burdick, & Lee, 2012). Additionally, based on our previous work, the BC/PAM DN gel was used as the template to in situ synthesize silver nanoparticles by an environmental friendly method, UV irradiation. A detailed characterization of the BC/PAM composite was done, and the effects of reaction conditions in the free radical polymerization were investigated on the microstructure, mechanical property and thermal stability of the composite. Furthermore, the influences of the templates, i.e., BC/PAM and pure BC were investigated on the AgNPs formation and the antibacterial activities of the corresponding silver impregnated nanocomposites, by the zone of inhibition and dynamic shake flask method, respectively.

2. Materials and methods

2.1. Bacterial strain and culture medium

Gluconacetobacter xylinus (formerly *Anisopodus xylinus*) (strain 1.1812) and *Staphylococcus aureus* (strain 1.128) were purchased from Institute of Microbiology Chinese Academy of Science and maintained on solid agar medium at 4 °C. Both the seed medium and the fermentation medium used for bacterial cellulose production contained 2.5% (w/v) mannitol, 0.3% (w/v) tryptone and 0.5% (w/v) yeast extract. Prior to autoclaving at 121 °C, the pH value of the medium was adjusted to 5.0.

2.2. Preparation and purification of BC film

The preparation of BC films was preformed according to our previous work (Yang et al., 2012a). Briefly, a single *G. xylinus* colony was transferred into 100 ml of seed culture medium and cultivated agitatedly for 24 h at 30 °C. Then, 6 ml of the cell suspension was introduced into a 250-ml Erlenmeyer flask containing 100 ml of fermentation culture medium, and incubated statically at 30 °C for 5 days. After that, the BC film was harvested and purified by boiling them in 1.0% NaOH solution for 2 h, and subsequently in distilled water for another 2 h. The two steps were repeated for three cycles. Finally, the film was thoroughly washed with distilled water until the pH of the washing liquid was neutral. The resulting BC films were of circular shape, 80 mm in diameter and 5 mm in thickness.

2.3. Synthesis of BC/PAM double-network gel

The as-prepared BC film was first partially dehydrated using mechanical press method, with the final thickness of the film was about 1/5 of the initial one. Then, the BC/PAM double-network gel was prepared by synthesis of PAM network within the BC gel using free radical polymerization method, with acrylamide (AM) as the monomer, *N*,*N*′-methylenebisacrylamide (MBA) as a crosslinker and ammonium persulfate (APS) as an initiator. In a typical experiment, the BC film was immersed in an aqueous solution of 1.0 mol/l AM containing 1.0 mol% MBA and 0.2 mol% APS for 24 h until reaching equilibrium. Subsequently, the BC film was picked out and transferred into a cell consisting of a pair of glass plates. The PAM network was polymerized within the BC gel at 60 °C for 6 h between two glass plates. After this polymerization process, the obtained BC/PAM DN gel was immersed in 500 ml distilled water for 3 d, the water being changed three times every day to remove low molecular weight components and allow the gel to swell.

2.4. In situ preparation of AgNPs impregnated BC/PAM nanocomposites

The BC/PAM DN gel, prepared under the condition of 1.0 mol/l AM, 1.0 mol% MBA and 0.2 mol% APS, was utilized as the template to in situ synthesize AgNPs. Typically, one piece of the BC/PAM film was immersed into 50 ml, 1 mM $AgNO_3$ solution under agitation at 100 rpm and 30 °C for 12 h protected from light, then were picked up and exposed to a UV lamp (wavelength = 254 nm, 30 W) for another 4 h. Subsequently, the film was washed with 3 × 10 ml of ultra-pure water to remove the excess chemicals. For comparison, pure BC was utilized as the template to in situ synthesize AgNPs according to the above-mentioned method.

2.5. Characterization

The morphology of both BC and BC/PAM films were observed by a JEOL, JSM-5600LV scanning electron microscope (Japan) with an acceleration voltage of 15 kV. Before observation, the films were freeze-dried and coated with a thin layer of gold. The mechanical properties of both BC and BC/PAM films were determined with a universal material testing machine (H5KS, Hounsfield Co., England) at a strain speed of 10 mm/min until the rupture of sample at 25 °C. Before test, the films were cut into an oblong shape of 1 cm width and 4 cm length. A total of eight measurements were performed for each sample. Tensile module E was determined by the average slope over the strain ratio of 0–10% from the stress–strain curve. The amount of silver in the nanocomposite was quantified by inductively coupled plasma (ICP) equipment (Prodigy, LEEMAN, USA) with the sample dissolved in 95% nitric acid. Transmission electron microscopy (TEM) images were recorded using a HITACHI, H-800 transmission electron microscope (Japan) operating at an acceleration voltage of 15 kV. For TEM measurements, samples were prepared by dropping 10–20 μl of finely ground BC/PAM-AgNPs or BC-AgNPs nanocomposite dispersions on a copper grid and dried under the heating lamp. The particle sizes of the AgNPs were measured using Image J software. At least 100 particles of each sample from different TEM images were analyzed. The histogram of the size distribution was established by Origin software. Thermogravimetric assay (TGA) was carried out with a NETZSCH TG 209 F1 analyzer equipment. The samples (ca. 5 mg) were put into ceramic pans and heated from 50 to 700 °C with a heating rate of 10 °C/min under nitrogen atmosphere. Derivative TG curves (DTG) were obtained to express the weight loss rate as a function of temperature.

2.6. Antibacterial test

The antibacterial activity of the BC/PAM-AgNPs or BC-AgNPs nanocomposite was determined against the common pathogenic bacteria *S. aureus*, which was pre-cultured at 37 °C to reach a concentration of 10^8 colony forming unit/ml (CFU/ml). Both nanocomposites were prepared according to the procedure in Section 2.4. All the samples were cut into circular discs (15 mm in diameter) for use. Two methods, i.e., the zone of inhibition and dynamic shake flask method were adopted to evaluate the antibacterial activity according to our previous work (Yang et al., 2012b). Briefly, the zone of inhibition method was performed to evaluate the antibacterial activity qualitatively by measuring the inhibition zone, i.e., the diameter of the nearest millimeter of the inhibited growth around the sample disk. At least 3 measurements were performed. The dynamic shake flask method was conducted to evaluate the antibacterial activity quantitatively. In this case, the samples were placed in contact with *S. aureus* liquid suspension

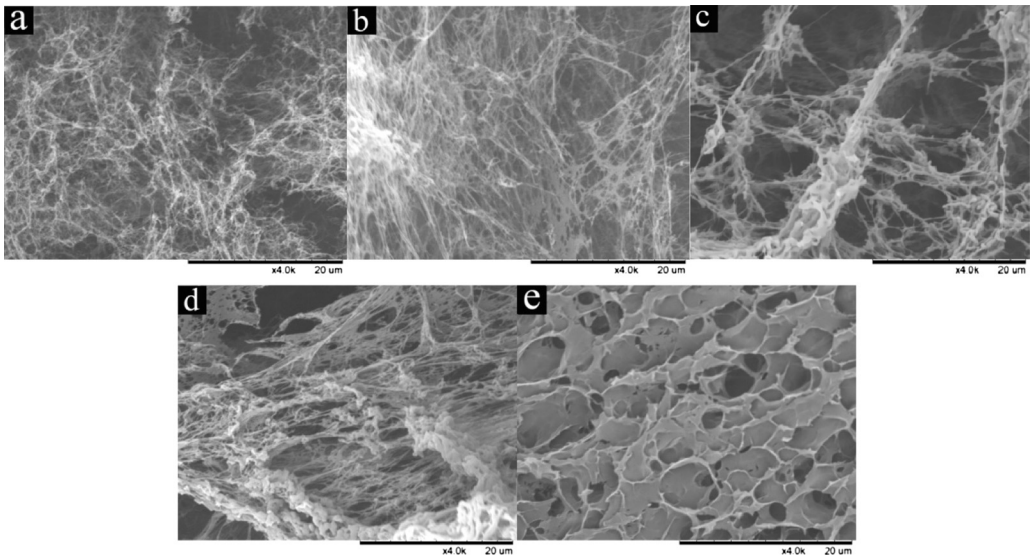

Fig. 1. SEM images of BC/PAM composites with different AM concentrations. (a) 0 mol/l; (b) 0.5 mol/l; (c) 1.0 mol/l; (d) 1.5 mol/l; (e) 2.0 mol/l.

and subjected to 160 rmp shaking at 37 °C. At 0 and 24 h contact times, the bacterial number (CFU) of the liquid suspension was determined by plating serial dilution on plate count agar. The same procedure was performed on BC/PAM or pure BC as control. The antibacterial effects of the samples were evaluated in three forms, i.e., bactericidal activity, bacteriostatic activity and killing ratio, and calculated using the following equations: Bactericidal activity = log CFU T_0 control − log CFU T_{24} composite; Bacteriostatic activity = log CFU T_{24} control − log CFU T_{24} composite; Killing ratio = (CFU T_{24} control − CFU T_{24} composite)/CFU T_{24} control × 100%, where CFU T_0 control and CFU T_{24} control meant the viable bacterial number for the control sample at 0 h and 24 h contact time, respectively, while CFU T_{24} composite represented the bacterial survival number for the BC/PAM-AgNPs or BC-AgNPs nanocomposite at 18 h contact time.

3. Results and discussion

3.1. Effects of AM concentrations on the microstructure of BC/PAM composite

Fig. 1 showed the SEM images of pure BC and BC/PAM composites with AM concentrations from 0.5 to 2.0 mol/l. In Fig. 1(a), the network structure of pure BC was clearly visible, and the BC microfibrils interlaced with each other to keep the porous structure well. For the BC/PAM composite, as shown in Fig. 1(b–e), when the AM concentration increased, the diameters of the BC microfibrils became larger since they were covered by more PAM, and the spaces between the BC network were filled by more PAM molecules. Specially, the BC microfibrils were embedded within the PAM layers at a high AM concentration of 2.0 mol/l. This indicated that the PAM penetrated into the BC network and formed a uniform composite structure. These modifications of BC microstructures were similar to other reported BC-polymer composites, such as BC-polyethylene glycol (Cai & Kim, 2010) and BC-polyvinyl alcohol (Qiu & Netravali, 2012).

3.2. Effects of AM concentrations on the thermal properties of BC/PAM composite

Fig. 2 showed the typical TG (a) and DTG (b) curves of BC/PAM composites prepared by different AM concentrations, with pure BC and PAM as control. For pure BC material, a quick drop in weight began at a temperature of about 257 °C, and the onset decomposition temperature (T_d) was 208 °C. As to pure PAM sample, two decomposition onset temperatures could be seen at approx. 200 and 366 °C, respectively, with the maximum rate of the corresponding decomposition ($T_{d,max}$) occurring at approx 219 and 388 °C,

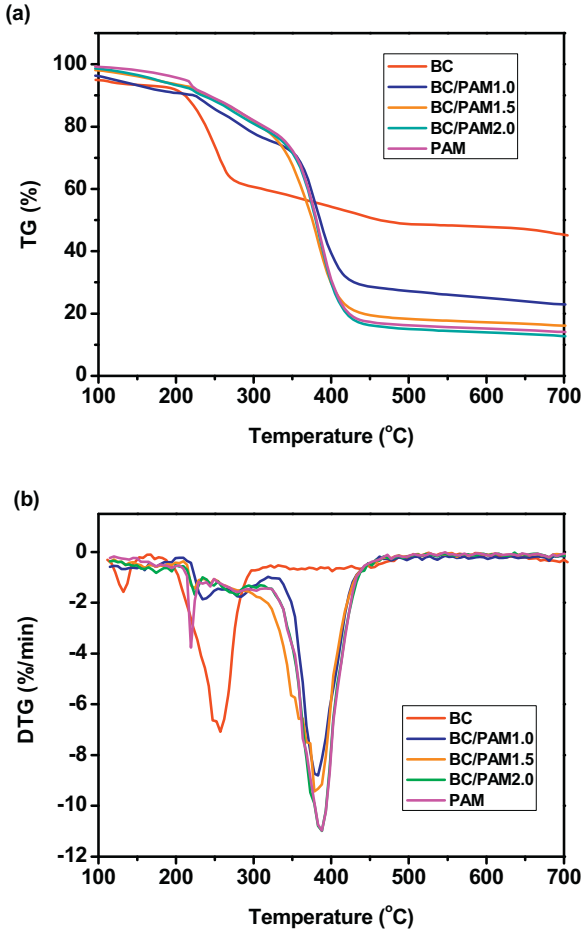

Fig. 2. TG (a) and DTG (b) curves of BC, PAM and BC/PAM composites with different AM concentrations.

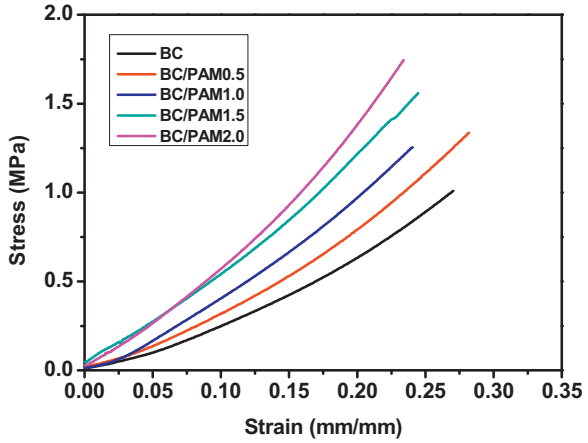

Fig. 3. Stress–strain curves of BC and BC/PAM composites with different AM concentrations. MBA concentration was 0.5 mol%.

respectively. It was obvious that the PAM material exhibited a much better thermal stability that BC. For the BC/PAM composites, both the T_d and $T_{d,\max}$ turned to a compromise value between that of pure BC and PAM, and they increased with a rising AM concentration. Specially, when the AM concentration rose to 2.0 mol/l, almost the same TG and DTG curves existed between pure PAM and BC/PAM composite. These results indicated that incorporation of PAM into the BC network could be helpful to improve the thermal stability of BC.

3.3. Effects of AM and MBA concentrations on the mechanical properties of BC/PAM composite

Figs. 3 and 4 showed the effects of the concentrations of AM monomer and MBA cross-linker, on the tensile strength of BC/PAM composites. The detailed data of tensile modulus, fracture stress and fracture strain were listed in Table 1. It could be seen that comparable with pure BC, BC/PAM composites displayed an increasing tendency in both the tensile modulus and fracture stress as the AM concentration increased. However, the tensile fracture strain decreased in the range of AM concentrations from 0.5 to 2.0 mol/l, and lower values comparable to pure BC were obtained at AM concentrations above 1.0 mol/l. The effects of MBA concentration on the tensile strength of BC/PAM composites were studied at a constant AM concentration of 1.0 mol/l. With higher cross-linking levels at MBA concentration above 0.50 mol%, the tensile modulus

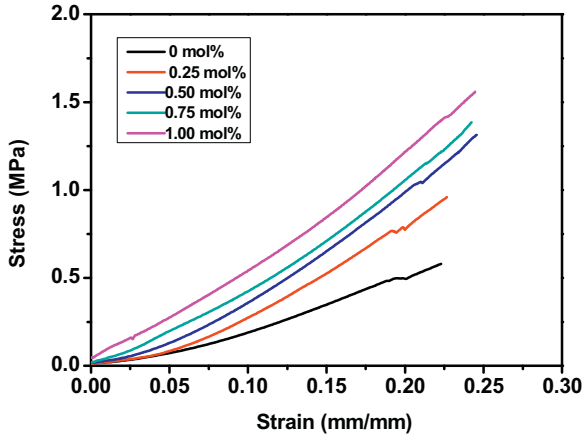

Fig. 4. Stress–strain curves of BC/PAM composites with different MBA concentrations. AM concentration was 1.0 mol/l.

Table 1
Effects of AM and MBA concentrations on the mechanical properties of BC/PAM composite.

Reaction conditions	Tensile modulus, E (MPa)	Tensile fracture stress (MPa)	Tensile fracture strain (mm/mm)
Pure BC	4.74	1.10	0.27
AM 0.5 mol/l*	4.95	1.16	0.30
AM 1.0 mol/l*	5.00	1.23	0.26
AM 1.5 mol/l*	5.23	1.37	0.26
AM 2.0 mol/l*	5.99	1.50	0.25
MBA 0 mol%**	2.80	0.52	0.23
MBA 0.25 mol%**	4.38	0.92	0.22
MBA 0.50 mol%**	5.00	1.23	0.26
MBA 0.75 mol%**	5.11	1.07	0.25
MBA 1.00 mol%**	5.23	1.07	0.25

* MBA concentration was 0.5 mol%, and APS concentration was 0.2 mol%.
** AM concentration was 1.0 mol/l and APS concentration was 0.2 mol%.

of the composite increased and reached up to higher values than that of pure BC. Both the fracture stress and fracture strain tended to increase for MBA concentration blow 0.50 mol%, while decrease at higher MBA concentrations above 0.50 mol%. This indicated that 0.50 mol% was a desirable value for MBA concentration.

3.4. Synthesis of BC/PAM-AgNPs naocomposite and its antibacterial activity

In our previous work, bacterial cellulose has been successfully utilized as the template to in situ synthesize AgNPs by different methods, such as chemical reduction with $NaBH_4$ as the reductant (Yang et al., 2012b) and hydrothermal treatment using bacterial cellulose as both the reducing and stabilizing agent, without any chemical reagents introduced (Yang et al., 2012a). It was found that the AgNPs synthesized on the BC matrix exhibited a small size and a narrow size distribution, e.g., 8.3 ± 3.6 nm and 17.1 ± 5.9 nm for the corresponding method, respectively. These results indicated that the structure of the three-dimensional network and large amount of the nanosized pores in the BC matrix acted as the nanoreactors for the nucleation and growth of the AgNPs. In this work, another environmentally benign and facile approach, UV irradiation was performed to produce AgNPs using both BC/PAM composite and pure BC as the template, with no chemical reagents introduced.

The size and size distribution of the AgNPs formed on BC/PAM composite and pure BC were analyzed by means of transmission electron microscopy (TEM) (Fig. 5), and the histogram based on the TEM images illustrated their average size and size distribution. The AgNPs synthesized on pure BC showed a smaller size than those on BC/PAM composite, with the values of 26.94 ± 1.56 nm and 68.01 ± 1.99 nm, respectively. Both the as-prepared AgNPs exhibited a round shape, which could be seen clearly from the inset images. The silver contents of both BC/PAM-AgNPs and BC-AgNPs nanocomposites were determined by elemental analysis using ICP, and the results were found to be 1.38% and 2.28%, respectively. By associating these results with the microstructures of BC and BC/PAM composite, it was thought that the smaller spaces in the BC/PAM composite might retard the Ag^+ penetration into the inner zone of the matrix and induce AgNPs loading intensively close to the surface zone, which resulted in a lower silver content and higher particle size of the AgNPs. Additionally, in this work, the AgNPs synthesized on pure BC exhibited a bigger particle size but similar silver content comparable with those by our previously reported method, e.g., hydrothermal treatment. The influences of different preparation methods of AgNPs based on the BC matrix as well as the reaction conditions will be discussed in our future work.

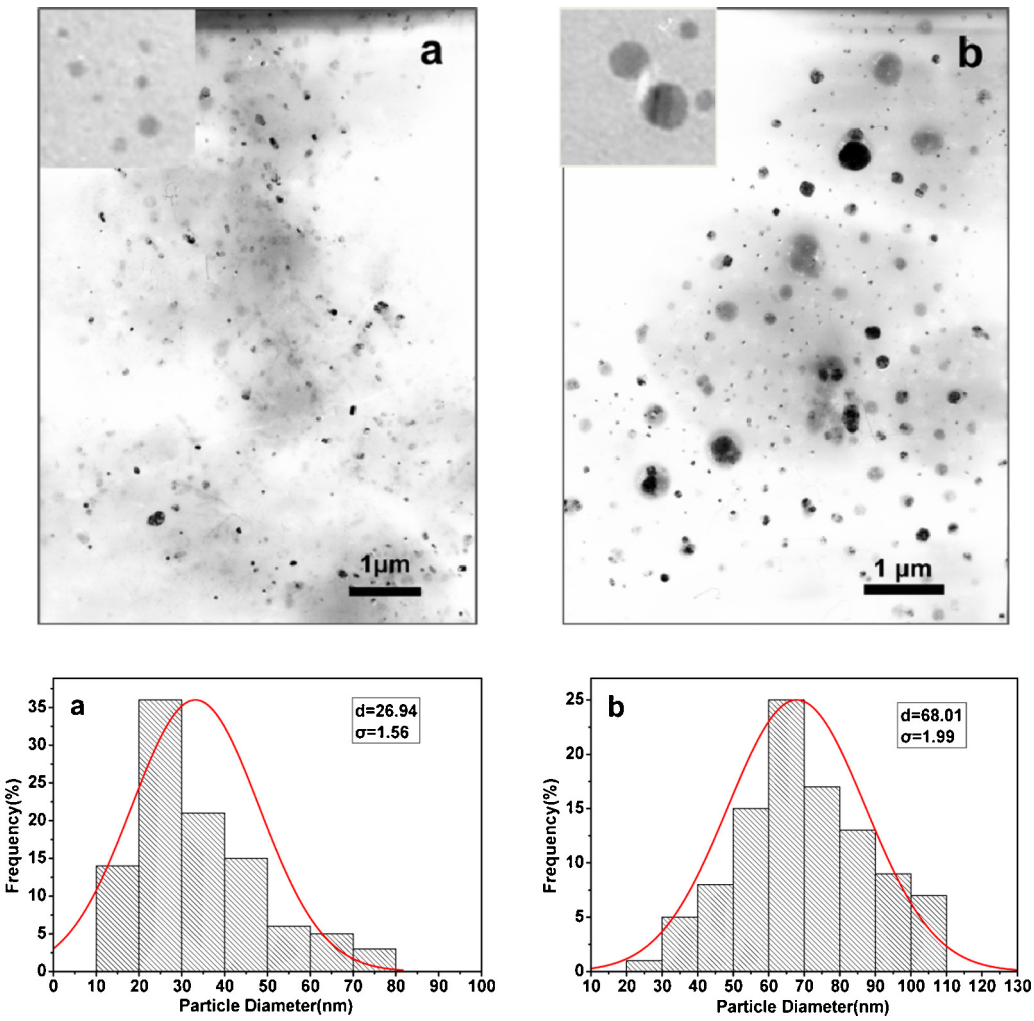

Fig. 5. The TEM images and particle size distribution histograms of silver nanoparticles formed in BC (a) and BC/PAM (b) composites. The inset showed the magnified images of AgNPs.

Comparisons of the antibacterial activities of both the BC/PAM-AgNPs and BC-AgNPs nanocomposites were tested against *S. aureus* by the zone of inhibition and dynamic shake flask method, respectively. In each test, the film samples were utilized with the same areas. For the zone of inhibition (seen in Fig. 6), two AgNPs impregnated nanocomposites exhibited obvious inhibition zones, while no inhibition zone was observed for the pure BC or BC/PAM matrix. This demonstrated that the antibacterial activity existed only due to silver nanoparticles but not the matrix itself. Moreover, a wider inhibition zone was obtained by BC/PAM-AgNPs than BC-AgNPs sample although the BC/PAM-AgNPs nanocomposite possessed a lower silver content. This might be attributed to the differences of the AgNPs distribution in the two matrices, that is to say, the AgNPs loaded close to the surface zone of the matrix was easy to release and hence produced a wider inhibition zone. For the quantitative assay of antibacterial activity, three parameters were calculated for comparison (Table 2). As seen from the data, although the BC/PAM-AgNPs nanocomposite possessed a lower silver content than BC-AgNPs, a close antibacterial effect reflected by three parameters was achieved by two silver containing nanocomposites. The reasons behind this phenomenon could also be found in the differences of the AgNPs distribution in the two matrices, which was referred above. Generally, low antibacterial activity was considered to be less than a 1-log reduction, moderate activity between a 1- and 3-log reduction, and high antibacterial activity was greater than a 3-log reduction (Gallant-Behm et al., 2005). Hence, it could be deemed that both the nanocomposites exhibited a high antibacterial effect, with the log reduction above 3 and the killing ratio above 99.9%.

Table 2
Quantitative antibacterial activity assay of BC-AgNPs and BC/PAM-AgNPs nanocomposites.

Samples	CFU T_0	CFU T_{24}	Bactericidal activity (log reduction)	Bacteriostatic activity (log reduction)	Killing ratio (%)
BC	1.07×10^8	2.52×10^8	–	–	–
BC-AgNPs	1.07×10^8	3.1×10^4	3.54	3.91	99.99
BC/PAM	1.07×10^8	2.06×10^8	–	–	–
BC/PAM-AgNPs	1.07×10^8	5.5×10^4	3.29	3.57	99.97

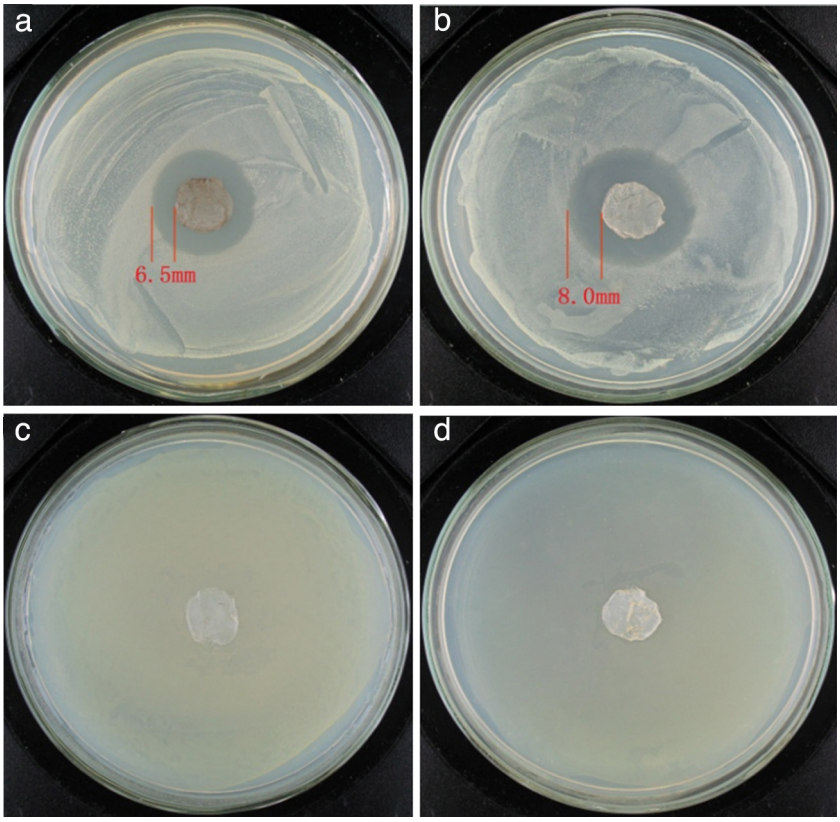

Fig. 6. Photograph images of the inhibition zone of BC/AgNPs (a) and BC/PAM-AgNPs nanocomposite (b) with pure BC(c) and BC/PAM (d) as control.

4. Conclusions

In this work, two matrices, BC/PAM composite and pure BC were utilized as the template to in situ synthesize silver nanoparticles by an environmental friendly method, UV irradiation. The influences of the templates were investigated on the AgNPs formation and antibacterial activities of the nanocomposites. It was found that, comparable to pure BC, the BC/PAM composite, which displayed a denser microstructure might retard the Ag^+ penetration into the inner zone of the matrix and induce AgNPs loading intensively close to the surface zone, thus producing a lower silver content, higher particle size of the AgNPs, as well as a wider inhibition zone by BC/PAM-AgNPs nanocomposite. For the quantitative assay of antibacterial activity, both the nanocomposites exhibited a high antibacterial effect, with the log reduction above 3 and the killing ratio above 99.9% after contact with *S. aureus* for 24 h. Additionally, in this work, the AgNPs synthesized on pure BC exhibited a bigger particle size but similar silver content comparable with those by our previously reported method, e.g., hydrothermal treatment. The influences of different preparation methods of AgNPs based on the BC matrix will be discussed in our future work.

Acknowledgments

The project was funded by the Chinese National Natural Science Foundation (no. 21004008), the Shanghai Municipal Education Commission and Shanghai Education Development Foundation ("Chen Guang" project, no. 11CG35), and the Fundamental Research Funds for the Central Universities. All the financial support is gratefully acknowledged.

References

Bao, L., Xu, Z., Li, R., & Li, X. (2010). Catalyst-free synthesis and structural and mechanical characterization of single crystalline $Ca_2B_2O_5 \cdot H_2O$ nanobelts and stacking faulted $Ca_2B_2O_5$ nanogrooves. *Nano Letters*, *10*, 255–262.

Bryaskova, R., Georgieva, N., Pencheva, D., Todorova, Z., Lazarova, N., & Kantardjiev, T. (2014). Synthesis and characterization of hybrid materials with embedded silver nanoparticles and their application as antimicrobial matrices for waste water purification. *Colloids and Surfaces A: Physicochemical and Engineering Aspects*, *444*, 114–119.

Buyanov, A. L., Gofman, I. V., Revel'skaya, L. G., Khripunov, A. K., & Tkachenko, A. A. (2010). Anisotropic swelling and mechanical behavior of composite bacterial cellulose–poly(acrylamide or acrylamide–sodium acrylate) hydrogels. *Journal of the Mechanical Behavior of Biomedical Materials*, *3*, 102–111.

Cai, J., Kimura, S., Wada, M., & Kuga, S. (2009). Nanoporous cellulose as metal nanoparticles support. *Biomacromolecules*, *10*, 87–94.

Cai, Z., & Kim, J. (2010). Bacterial cellulose/poly(ethylene glycol) composite: Characterization and first evaluation of biocompatibility. *Cellulose*, *17*, 83–91.

Cheng, K. M., Hung, Y. W., Chen, C. C., Liu, C. C., & Young, J. J. (2014). Green synthesis of chondroitin sulfate-capped silver nanoparticles: Characterization and surface modification. *Carbohydrate Polymers*, *110*, 195–202.

Czaja, W., Krystynowicz, A., Bielecki, S., & Brown, R. M. (2006). Microbial cellulose—The natural power to heal wounds. *Biomaterials*, *27*, 145–151.

El-Rafie, M. H., Ahmed, H. B., & Zahran, M. K. (2014). Characterization of nanosilver coated cotton fabrics and evaluation of its antibacterial efficacy. *Carbohydrate Polymers*, *107*, 174–181.

Gallant-Behm, C. L., Yin, H. Q., Liu, S., Heggers, J. P., Langford, R. E., Olson, M. E., et al. (2005). Comparison of in vitro disc diffusion and time kill-kinetic assays for the evaluation of antimicrobial wound dressing efficacy. *Wound Repair and Regeneration*, *13*, 412–421.

Gong, J. P., Katsuyama, Y., Kurokawa, T., & Osada, Y. (2003). Double-network hydrogels with extremely high mechanical strength. *Advanced Materials*, *15*, 1155–1158.

Hagiwara, Y., Putra, A., Kakugo, A., Furukawa, H., & Gong, J. P. (2010). Ligament-like tough double-network hydrogel based on bacterial cellulose. *Cellulose*, *17*, 93–101.

Jiang, P., Zhou, J., Li, R., Wang, Z., & Xie, S. (2006). Poly(vinyl pyrrolidone)-capped five-fold twinned gold particles with sizes from nanometres to micrometres. *Nanotechnology*, *17*, 3533–3538.

Jiang, P., Zhou, J., Li, R., Gao, Y., Sun, T., Zhao, X., et al. (2006). PVP-capped twinned gold plates from nanometer to micrometer. *Journal of Nanoparticle Research*, *8*, 927–934.

Lee, S. W., Tettey, K. E., Kim, I. L., Burdick, J. A., & Lee, D. (2012). Controlling the cell-adhesion properties of poly(acrylic acid)/polyacrylamide hydrogen-bonded multilayers. *Macromolecules*, *45*, 6120–6126.

Li, R., Bao, L., & Li, X. (2011). Synthesis, structural, optical and mechanical characterization of SrB_2O_4 nanorods. *CrystEngComm*, *13*, 5858–5862.

Loher, S., Schneider, O. D., Maienfisch, T., Bokorny, S., & Stark, W. J. (2008). Micro-organism-triggered release of silver nanoparticles from biodegradable oxide carriers allows preparation of self-sterilizing polymer surfaces. *Small*, *4*, 824–832.

Qiu, K., & Netravali, A. (2012). Bacterial cellulose-based membrane-like biodegradable composites using cross-linked and noncross-linked polyvinyl alcohol. *Journal of Materials Science*, *47*, 6066–6075.

Rai, M., Yadav, A., & Gade, A. (2009). Silver nanoparticles as a new generation of antimicrobials. *Biotechnology Advances*, *27*, 76–83.

Saleh, R., & Djaja, N. F. (2014). Transition-metal-doped ZnO nanoparticles: Synthesis, characterization and photocatalytic activity under UV light. *Spectrochimica Acta, A: Molecular and Biomolecular Spectroscopy*, *130*, 581–590.

Yang, G., Xie, J., Deng, Y., Bian, Y., & Hong, F. (2012). Hydrothermal synthesis of bacterial cellulose/AgNPs composite: A green route for antibacterial application. *Carbohydrate Polymers*, *87*, 2482–2487.

Yang, G., Xie, J., Hong, F., Cao, Z., & Yang, X. (2012). Antimicrobial activity of silver nanoparticle impregnated bacterial cellulose membrane: Effect of fermentation carbon sources of bacterial cellulose. *Carbohydrate Polymers*, *87*, 839–845.